Science of the Total Environment 543 (2016) 851–861

Contents lists available at ScienceDirect

Science of the Total Environment

journal homepage: www.elsevier.com/locate/scitotenv

Soil–plant interaction monitoring: Small scale example of an apple orchard in Trentino, North-Eastern Italy

Giorgio Cassiani [a,*], Jacopo Boaga [a], Matteo Rossi [a], Mario Putti [b], Giuseppe Fadda [b], Bruno Majone [c], Alberto Bellin [c]

[a] Dipartimento di Geoscienze, Università di Padova, Italy
[b] Dipartimento di Matematica, Università di Padova, Italy
[c] Dipartimento di Ingegneria Civile e Ambientale, Università di Trento, Italy

HIGHLIGHTS

- A novel noninvasive geoelectrical system is proposed for root water uptake monitoring.
- The approach is applied to an apple orchard in Northern Italy.
- Results indicate the need to consider also pore water electrical conductivit.

ARTICLE INFO

Article history:
Received 10 January 2015
Received in revised form 11 March 2015
Accepted 26 March 2015
Available online 2 April 2015

Keywords:
Hydrogeophysics
Irrigation experiments
Vadose zone
Root activity

ABSTRACT

Accurate monitoring and modeling of soil–plant systems are a key unresolved issue that currently limits the development of a comprehensive view of the interactions between soil and atmosphere, with a number of practical consequences including the difficulties in predicting climatic change patterns. This paper presents a case study where time-lapse minimal-invasive 3D micro-electrical tomography (ERT) is used to monitor rhizosphere eco-hydrological processes in an apple orchard in the Trentino region, Northern Italy. In particular we aimed at gaining a better understanding of the soil–vegetation water exchanges in the shallow critical zone, as part of a coordinated effort towards predicting climate-induced changes on the hydrology of Mediterranean basins (EU FP7 CLIMB project). The adopted strategy relied upon the installation of a 3D electrical tomography apparatus consisting of four mini-boreholes carrying 12 electrodes each plus 24 mini-electrodes on the ground surface, arranged in order to image roughly a cubic meter of soil surrounding a single apple tree. The monitoring program was initially tested with repeated measurements over about one year. Subsequently, we performed three controlled irrigation tests under different conditions, in order to evaluate the water redistribution under variable root activities and climatic conditions. Laboratory calibration on soil samples allowed us to translate electrical resistivity variations into moisture content changes, supported also by in-situ TDR measurements. Richards equation modeling was used also to explain the monitoring evidence. The results clearly identified the effect of root water uptake and the corresponding subsoil region where active roots are present, but also marked the need to consider the effects of different water salinity in the water infiltration process. We also gained significant insight about the need to measure quantitatively the plant evapotranspiration in order to close the water balance and separate soil structure effects (primarily, hydraulic conductivity) from water dynamics induced by living plants.

1. Introduction

In recent years a growing attention has been attracted by the importance of understanding and characterizing the manifold processes that take place in the so called Earth's "Critical Zone" (ECZ) as defined by the U.S. National Research Council (2001). The ECZ represents the thin veneer of our planet from the top of the tree canopy to the bottom of drinking water aquifers. Being at the interface between the planet and its atmosphere, the ECZ is a complex natural reactor, where inputs of solar energy, atmospheric deposition and gas fluxes interact with the biota and rock mass to maintain soil, nourish ecosystems and accumulate and exchange water (Anderson et al., 2004; Brantley et al., 2006). This diversity of interactions presents an enormous scientific challenge to understanding the linkages and chain of impacts. In particular, within the ECZ, the interactions between soil, plants and atmosphere (SPA)

* Corresponding author.

http://dx.doi.org/10.1016/j.scitotenv.2015.03.113
0048-9697/

play a fundamental role in the exchanges of mass (especially water and CO_2) and energy, that in turn control a number of environmental processes of the highest general interest, including those affecting and mitigating climatic changes. Terrestrial vegetation modulates and sustains evapotranspiration (ET) and precipitation. ET has been termed "green water" flow (Falkenmark and Rockstro¨m, 2004). Root-zone soil moisture is the major stock of green water. Soil moisture affects biota directly, by controlling the availability of resources for organisms, and indirectly, by modifying abiotic processes that affect ecosystem dynamics. Green water stocks and flows are affected by biological processes, primarily mediated by plants, with multiple feedbacks from soil and atmosphere, thereby affecting surface energy and water-vapor fluxes, boundary layer dynamics, precipitation, and soil moisture regime (e.g., Bonan, 2002). On a larger scale, the response of terrestrial ecosystems to global change is often mediated or sustained by changes in soil moisture dynamics (Rodriguez-Iturbe and Porporato, 2005). Climate warming enhances ET, thereby accelerating the hydrologic cycle, and climate change research predicts changes in both the mean and the variance of hydrological drivers (Easterling et al., 2000). Also of great impact is the understanding of the relevant processes taking place in agricultural practice, in order to optimize irrigation and plant resilience in face of expected climatic changes and growing population demands ("more crop per drop", Tilman et al., 2001; Howden et al., 2007).

In spite of the scientific challenges described above, the understanding of complex SPA interactions is still limited, particularly regarding the subsoil components, including root activities, and their changing states, mainly by the lack of spatially extensive and time intensive data. Common point-based methods do not allow the investigation of state variables' spatial distribution. Remote sensing techniques generally penetrate the subsoil only by a few centimeters and their view of the subsurface is hindered by the vegetation itself.

To fill this knowledge gap, innovative non-invasive and spatially extensive techniques are more and more often called into play (Jayawickreme et al., 2014). Ground-based, non-invasive (geophysical) techniques such as Electro-Magnetic methods, Ground Penetrating Radar (GPR) and Electrical Resistivity Tomography (ERT) have been increasingly applied at different scales to image static and dynamic characteristics of the subsoil, particularly for hydrological purposes (Vereecken et al., 2006; Binley et al., 2011). Recently, these techniques have also been used for dynamic hydro-biological characterization (e.g. Wiley et al., 2010). The use of non-invasive techniques, GPR and ERT in particular, can be considered state-of-the-art for the estimation of moisture content changes (Binley et al., 1996, 2002; Deiana et al., 2007). However, the application of these techniques to the very small scale and at the resolution needed for SPA interactions is not a trivial technical task, so that the use of these techniques for investigation at the root-zone scale is still in its infancy. In addition, the interpretation of the results in terms of soil dynamics has non-trivial intricacies, involving moisture content, pore water salinity and temperature [e.g., Cassiani et al., 2012; Ursino et al., 2014].

In the framework of plants/subsoil interactions, ERT has been downscaled to image the root zone geometry (Amato et al., 2008; Werban et al., 2008; Petersen and al Hagrey, 2009; Nijland et al., 2010; al Hagrey and Petersen, 2011; Robinson et al., 2012). Similarly, GPR has been used to try and identify particularly the root structure in the shallow subsoil (Butnor et al., 2001; Leucci, 2010; Bassuk et al., 2011). However, neither GPR nor ERT has been proven to be fully capable of identifying the details of the small-scale root system structure, even though some success has been reported in specific cases (Rossi et al., 2011; Wu et al., 2014). This is indeed not surprising, as geophysical techniques can only sense the spatial patterns or the temporal changes in the physical parameters they measure, so contrasts in physical properties between roots and the surrounding soil are needed to detect roots per se. This lucky situation rarely takes place, at least using electrical or electromagnetic methods that are by far the most used techniques for this purpose. Therefore the identification of root geometry and the quantification of root mass, that could have important consequences for carbon sequestration assessments, remains largely an unresolved issue.

A different approach is to try and quantify root water uptake (RWU) from changes in soil moisture content and consequently from changes in geophysical quantities that depend on that, such as electrical resistivity and dielectric constant. From this information one can draw conclusions about mass and energy transfers between soil and atmosphere as mediated by plants. Examples of this approach date back at least a decade, with a recent growing interest (Michot et al., 2003; Jayawickreme et al., 2008, 2010; Beff et al., 2013; Macleod et al., 2013; Boaga et al., 2014; Cassiani et al., 2015; Shanahan et al., 2015). Generally speaking, such an approach is a particular case of more general hydro-geophysical methods and a full exploitation of the data information content can be expected if data and modeling are used jointly, for instance using advanced Data Assimilation techniques (see e.g. Hinnell et al., 2010; Camporese et al., 2011, in press; Manoli et al., 2015).

The EU FP7 project CLIMB (Climate Induced Changes on the Hydrology of Mediterranean Basins — Ludwig et al., 2010) had among its goals the reduction of uncertainty in the prediction of climate change impacts on the hydrology of Mediterranean basins. One of the study areas was the Noce river catchment in Trentino, North-Eastern Italy. The lower river catchment (Val di Non) is a region of intensive apple production. Therefore knowledge of the apple tree orchards' water dynamics is key to the understanding of the local hydrology, especially as apple trees require a very intense irrigation during summer time. Therefore we focused our attention on the root/vadose zone description of the apple tree orchards. This area of investigation posed new, demanding, interdisciplinary challenges among which is the collection and interpretation of spatially extensive and time intensive non-invasive data that can greatly contribute towards the understanding of the soil–plant–atmosphere interaction at an unprecedented scale and resolution.

In this paper we present the results of the very small-scale ERT acquisitions around a single apple tree in the Val di Non. We conducted monitoring of both long term natural changes and controlled irrigation experiments, in order to assess value, strengths and limitations of the non-invasive techniques for root/vadose zone monitoring. The main goals of this study were:

(a) to study the small scale dynamics of moisture content in an apple orchard where irrigation is the main source of water during the growing season;
(b) to test and validate the capabilities of small-scale ERT for the monitoring of eco-hydrological processes at the small scale, where processes of primary interest for soil–plant–atmosphere interactions take place;
(c) to assess the value of unsaturated flow modeling in supporting and validating the conclusions drawn on the basis of time-lapse hydro-geophysical monitoring.

2. The test site

The experimental site is an apple orchard located at Maso Maiano, near Cles, in 'Val di Non' valley, Trentino (Fig.1). 'Val di Non' is a mountain region widely known for apple production. The orchard has an area of roughly 5000 m^2 with an elevation of about 640 m.a.s.l. There are about 1200 apple trees (cultivar Golden Delicious) planted in 2004 along North–south rows spaced about 3.5 m. Plants are placed at about 1 m from each other along each row and the canopy height is about 2.5 m. The apple trees have an average stem diameter of approximately 0.04 m. In the field the soil surface is managed with a grass cover. The site is located on a moraine versant of an ancient Wurmian glacier valley and the soil is a heterogeneous glacial deposit, with stones

and pebbles in a sandy–silty matrix with practically no clay fraction and is classified as a sandy loam.

A single apple tree, about 1.8 m high, was selected for detailed 3D time-lapse monitoring of the soil dynamics using electrical resistivity tomography (ERT). The adopted acquisition geometry was similar to the one implemented by Cassiani et al. (2009) to monitor infiltration processes along a hillslope, but adapted in order to maximize resolution in the tree root zone, thus focusing on about a cubic meter of soil surrounding the apple tree. Four micro-boreholes bearing electrode strings were assembled using PVC tubes and stainless steel ring electrodes (Fig. 2). All wiring was placed internally in the tube. Each borehole is composed of 12 electrodes spaced 8 cm, all made with folded stainless steel foil, and 3 cm high. Once assembled, each string takes the form of a 1.2 m long pole having a 1 inch. diameter that was driven into the ground, with the help of some pre-drilling with a smaller diameter. Each pole was installed by percussion, avoiding excessive soil disturbance and permitting an excellent contact between soil and electrodes. The four boreholes were placed at the corners of a square having 0.9 m side. In addition to the 48 borehole electrodes, we also placed 24 electrodes regularly spaced (about 0.1 m) at the ground surface. The field setup is shown in Fig. 2a, and the electrode geometry is detailed in Fig. 3.

In order to have a direct measurement of soil moisture content, a 30 cm TDR probe (see Fig. 3) was placed vertically in the soil in proximity of the tree trunk, and repeated measurements were taken utilizing a Tektronix 1502 time-domain reflectometer.

3. Data acquisition and processing methodology

The goal of the time-lapse 3D ERT acquisitions was to allow high resolution monitoring of soil–plant interactions in the root zone. All acquisitions were performed using a 72-electrode IRIS Syscal Pro resistivimeter, trying to exploit at its best the speed of the 10 parallel physical channels of the instrument, in order to capture the dynamics of the potentially fast infiltration processes in the shallow vadose zone around the tree. At the same time, maximal resolution was sought, in order to picture the root water uptake and infiltration patterns in their potentially complex 3D structure. Both requirements above are satisfied adopting for all measurements a full 72 channel skip 0 dipole–dipole acquisition (i.e. each dipole is composed of electrodes next to each other in the numbering sequence, and thus also with minimal mutual distance) as done e.g. by Cassiani et al. (2009). We acquired both the direct and reciprocal configurations, in order to assess the reciprocal error as an estimate of measurement error (see e.g. Cassiani et al., 2006). In the quality control phase we only retained data that pass the 5% reciprocal error criterion at all measurement times. This in general saved around 80% of the about 2400 quadripoles (twice as much if we consider also reciprocals) used in the acquisition.

Data were inverted to produce the 3D resistivity volumes using the R3T code by A. Binley (2011) using a very fine triangular prism elements of 0.025 m side for the inner zone (Fig. 3), while larger mesh cells were used for the background extending well beyond and below the ERT control volume surrounded by the boreholes (2 m in the horizontal directions 3 m in depth).

Of particular interest are, in this context, the time-lapse resistivity changes that can be linked, primarily, to changes in soil moisture content. In order to enhance the changes from one time frame to the next, a ratio inversion approach was adopted (Daily et al., 1992) were for each quadripole the data to be inverted at each time step are constructed from the ratio of resistances of that same quadripole in the current time step and in the reference (initial) time step (see e.g. Cassiani et al., 2006, for more details). Ratio inversion is a powerful approach to highlight subtle time-lapse variations of electrical conductivity that would be otherwise overwhelmed by error differences in subsequent absolute resistivity images (Daily et al., 1992). The results are consequently given in terms of resistivity ratios with respect to the initial reference state. For details about the methodology consider e.g. Binley and Kemna (2005).

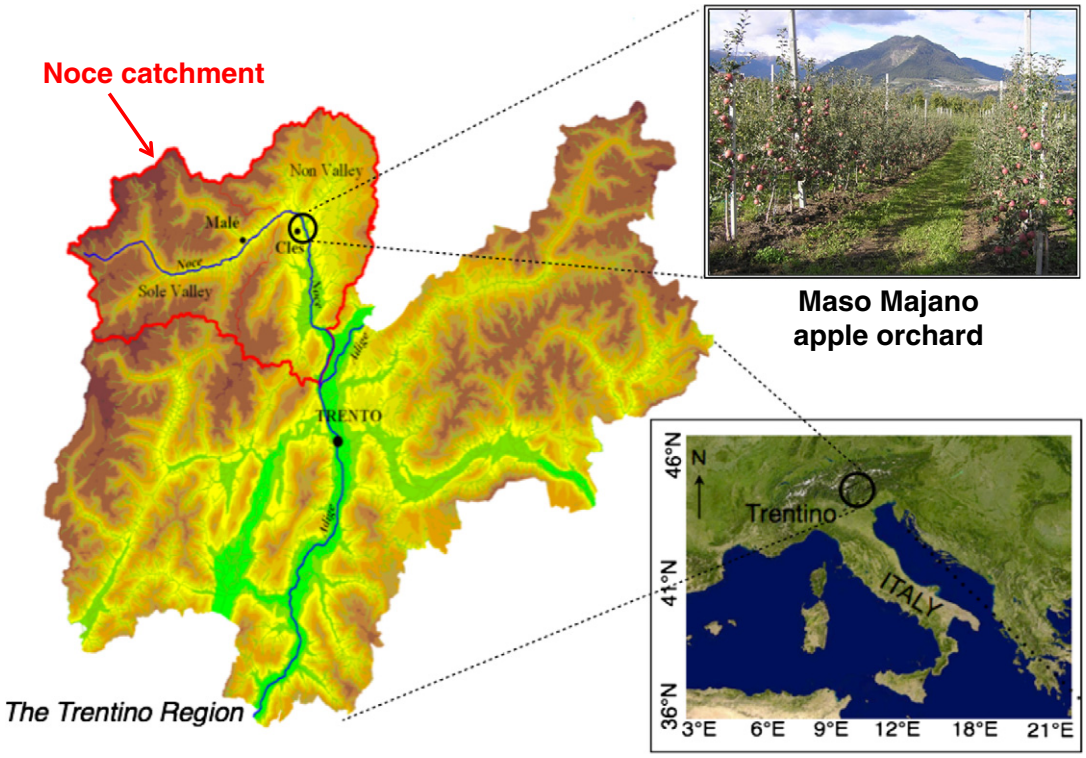

Fig. 1. The Maso Majano test site is located in the Alpine region of Northern Italy. The site is located in an apple orchard.

Fig. 2. Details of the micro-boreholes installed at the Maso Majano test site (b) and of their field deployment (a).

4. Results

We conducted repeated ERT measurements at the Maso Majano site for about two years (see Table 1). Changes of electrical resistivity over time, especially in different seasons, were quite apparent. However, the relatively coarse time sampling between different measurements (see Table 1) does not allow to reconstruct reliably the soil moisture content dynamics. In this paper, therefore, we concentrate our attention on the results of the three irrigation experiments conducted at the site, under different seasonal conditions and partly using different irrigation patterns:

- In August 2011, a drip irrigation under the dry summer conditions;
- in May 2012, a sprinkler irrigation in very wet conditions during the dynamic spring growing season on the apple tree;
- In November 2012, a second sprinkler irrigation, again in wet conditions, but with the limited autumn plant activity.

The three experiments were planned to examine the effects of the different types of irrigation schemes during different climatic conditions, and the impact of the apple tree RWU at different stages of its annual physiological cycle.

4.1. Irrigation test of August 2011

The soil conditions in August 2011 were very dry (moisture content about 12% at the start of the irrigation experiment) as a consequence of a long rainless period preceding the experiment. In addition, the monitored apple tree had been excluded from the irrigation system for the two weeks preceding the experiment, and the soil surface had been covered with a plastic sheet to limit direct exchanges to the atmosphere.

The irrigation test was conducted using the two drippers (located as indicated in Fig. 4) that are generally used during the summer irrigation period to water the same tree, using also the same irrigation scheme and rate with 6 h irrigation and at a total rate of 2.4 l/h. Therefore the results of this test are representing the standard working conditions of the system during summer. Fig. 4 shows the time-lapse ERT resistivity ratio volumes obtained at four different time instants after irrigation started, and related to the background conditions before irrigation. The effect of the drippers is very clear in these images. The regions where resistivity changes are limited to the surrounding of the two drippers, and the water seems to penetrate no more than 30 to 40 cm below the ground surface. Of course it is practically impossible to establish, from these images, whether RWU is active and to what extent it limits the penetration apparent water content change to further depths. But we can at least conclude that in water is not reaching any deeper in the subsurface as a consequence of standard irrigation at the site. Therefore it is very likely that active roots are not extending much deeper than the observed maximum depth of electrical resistivity changes in these images. Note that the practiced irrigation scheme is likely to influence the growth of the root system, so we expected the active roots to be to a large extent aligned with the dripper alignment.

A close examination of the evolution of the water plumes after irrigation ends (Fig. 4) seems also to indicate a reduction in the amount of water present in the system, with changes back to the original dry conditions and no further spreading of the plumes, as expected in presence of localized RWU on the proximity of the drippers and limited to a rather shallow depth. However, this experiment alone could not provide any more direct evidence of the extent of the RWU zone.

4.2. Irrigation test of May 2012

The second irrigation experiment was conducted in early May 2012, i.e. at the peak of the Spring growing season. Contrary to the previous

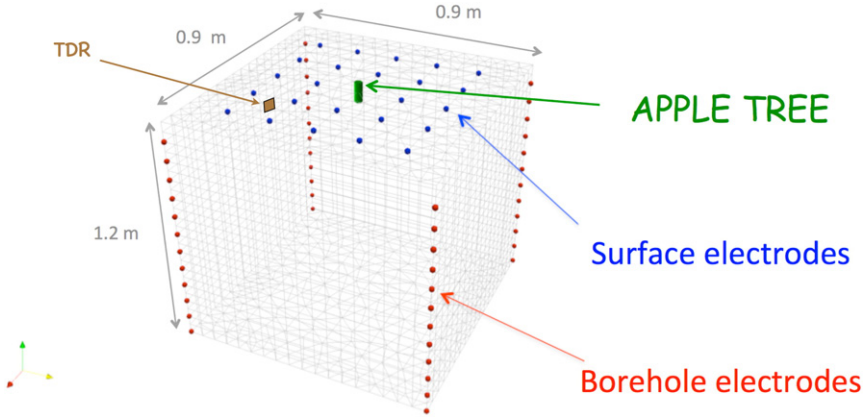

Fig. 3. Electrode geometry around the apple tree in the Maso Majano orchard, and the inner part of the 3D mesh used for ERT inversion. In brown the TDR position.

Table 1
Dates of 3D ERT monitoring at the Maso Majano test site, with particular evidence given to the three irrigation tests described in this paper.

Date	Note
15/10/10	Installation and measurement 1
14/01/11	Measurement 2
04/04/11	Measurement 3
28/04/11	Measurement 4
18/05/11	Measurement 5
06/07/11	Measurement 6
04/08/11	Measurement 7 + Irrigation test
07/09/11	Measurement 8
05/10/11	Measurement 9
03/05/12	Measurement 10 + Irrigation test
04/11/12	Measurement 11 + Irrigation test

experiment, in this case we started from a wet soil condition (about 28% moisture content, see the TDR data in Fig. 5), as a consequence of very abundant precipitations during April 2012. The weather during this experiment was hot and sunny (26 °C at noon), with expected very intense evapotranspiration.

In order to highlight features that could not be observed using the standard dripper irrigation scheme previously used, in this case we used a sprinkler with a much higher flow rate (3.3 l/min) for a total of 150 min and a volume of about 500 l. Practically this entire water volume was spread upon the surface of the ERT control volume, and no ponding was observed at the surface for the entire duration of the experiment. Irrigation started at 10:15 a.m., thus we could follow the evolution of soil moisture content for the entire day, and particularly at the peak of daily temperature and evapotranspiration.

Given the wet initial conditions, our ERT monitoring was not expected to identify easily the irrigation wetting front, since the corresponding resistivity contrasts were likely to be small. Rather, we expected to image the effects of the strong evapo-transpiration caused by the plant at the peak of its growing season and during the hottest time of the day. In fact, Fig. 6 shows a progressively larger and larger more resistive zone expanding around a depth of 30 cm from the surface, where most plant root activity is expected (e.g. de Silva et al., 1999). Resistivity increases substantially with respect to the initial condition, even though a substantial amount of water has been added to the system in the meanwhile. This is hardly surprising, as similar phenomena have been observed elsewhere, even in more extreme conditions (Boaga et al., 2014). The maximum increase in resistivity is observed at the time of peak air temperature in the early afternoon. The dipole–dipole acquisition lasted around 20 min for each time step and the irrigation experiment lasted few hours. In these conditions we can exclude temperature variations able to generate the strong electrical signal differences recorded (Jayawickreme et al., 2008). Fig. 7 shows also that the shape of zone with increasing resistivity is also correlated to the location of the drip system that is normally used for irrigation — see Fig. 4 for comparison. Indeed the region where resistivity has increased seems to delineate the volume where RWU has taken place — consider Fig. 7 that corresponds to the situation at about 19:00 h, i.e. when evapotranspiration has practically ceased and the total 3D extent of the more resistive zone is mapped. This piece of evidence confirms that the RWU zone is located in correspondence of the location of the line of drippers used for standard irrigation.

4.3. Irrigation test of November 2012

Finally, a further irrigation test was run in November 2012. This was an even wetter period, as normally observed in the Alpine climatic conditions, with an initial soil moisture content as high as 37% (measured by the installed TDR). The starting conditions, in terms of absolute resistivity values, are shown in Fig. 8. In this figure we show particularly the resistivity distribution at three depth slices, showing essentially a fairly high and homogeneous electrical conductivity distribution, with the sole exception of a shallow more resistive (presumably, drier) layer. At this time of the year, following harvest, the plant is much less active than in May. Again the same TDR and ERT monitoring was applied to a sprinkler irrigation experiment, for a total of 500 l applied with a lower rate equal to 100 l/h for 5 h. In spite of this large amount of water, the TDR data show (Fig. 9) that the soil moisture content can only increase only slightly to 46% as an effect of irrigation, and decreases very slowly afterwards.

The corresponding 3D distribution of resistivity change with respect to background, from ERT, is also shown in Fig. 10. Two features of these images are apparent:

(a) ERT detects a resistivity decrease at the surface, as an effect of the increased water content caused by irrigation. This increase is observed, with diminishing intensity, down to a depth of roughly 50 cm from the ground surface;
(b) at the same time, ERT images an increase in electrical resistivity in the deeper region (below 50 cm) and this increase takes place already half an hour from the start of the irrigation,

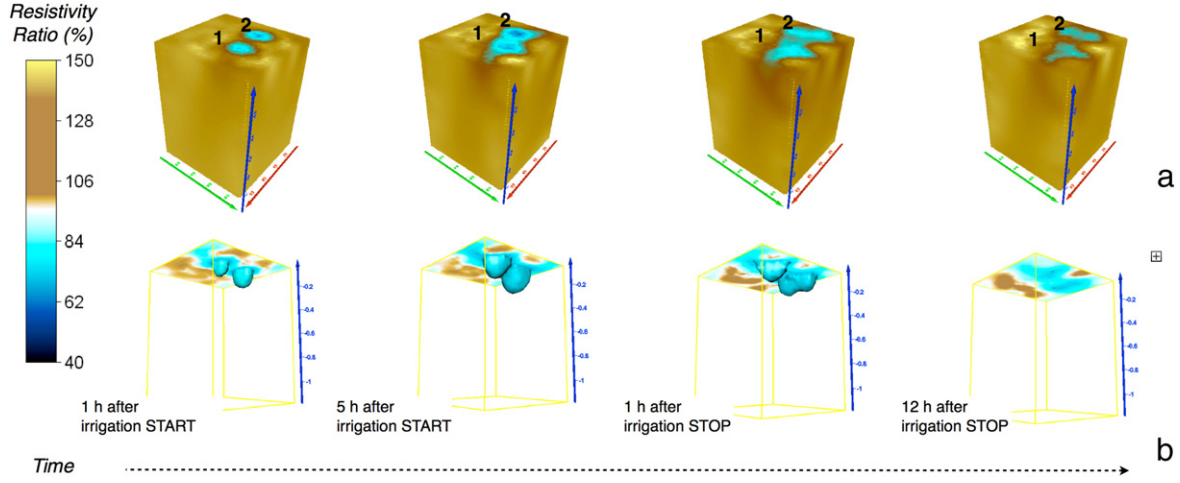

Fig. 4. August 2011 experiment: resistivity ratio with respect to background at four time steps. In (a), 1 and 2 indicate the locations of the two drippers. In (b) we show the iso-surface equal to 70% of the background resistivity: this level does not penetrate any deeper than 30–-40 cm below ground surface.

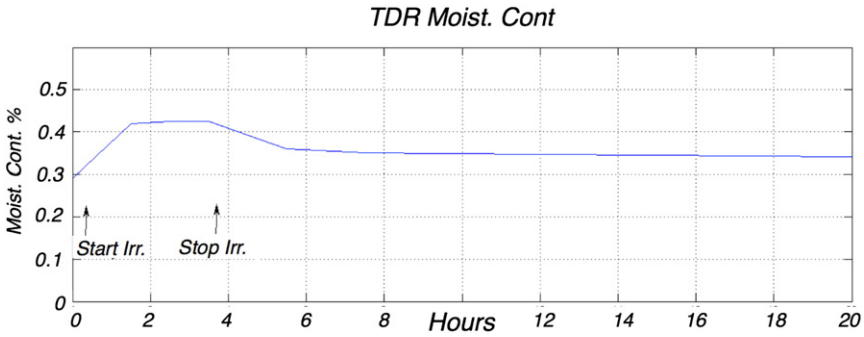

Fig. 5. May 2012 experiment. Moisture content measured by TDR in the top 30 cm. Note how the moisture content was already high at the start of the experiment.

remaining largely unchanged in the following time steps albeit with some smoothing and redistribution, till the end of monitoring.

We are confident of the inversion results due the very high ERT resolution for the volume of interest (48 buried electrodes plus 24 surface electrodes for less than 1 m^3). We observe these deeper anomalies in a region crossed by the boreholes where electrodes are placed. Close to the electrodes we have the highest sensitivity in the inversion process. Therefore we can confidently exclude that these deep features are inversion artifacts. Considering this, explaining these results in terms of hydrological processes is posing more challenges than for the previous experiments. Evapo-transpiration is not likely to be a strong mechanism in November, with a maximum daily temperature around 10 °C. Thus the resistivity increase at a depth exceeding the expected depth of the root apparatus (60 cm) cannot be attributed to suction decreasing the soil moisture content. Some other mechanisms must be called into play.

5. Discussion and interpretation

The data collected at Maso Majano and summarized in the section above pose a severe challenge to a simplified interpretation. In particular, while the data of August 2011 and May 2012 are possibly justifiable in terms of moisture content changes only, so it is not the case for the November 2012.

In order to clarify the structure of the observed phenomena, we averaged the resistivity ratio blocks for the two 2012 surveys (see Figs. 6 and 10) along horizontal planes and produced 1D vertical profiles that are much simpler to analyze (Figs. 11 and 12). In both cases we present the situation at two time steps, at 0.5 and 2.5 h since the start of irrigation. Note that the two figures present scenarios that are not fully comparable, as the irrigation rate was three time slower in November with respect to May, and the initial conditions were also rather different, even though wet in both cases. Nevertheless a visual comparison of the two scenarios reveals a couple of interesting features:

- At the beginning of both experiments (0.5 h) the shallow subsoil sees a reduction in resistivity that reaches a value around 50% of the background value right at the surface. This is of course compatible with soil wetting. The wetting front at 0.5 h is of course deeper in the May experiment, as the irrigation rate was higher. At this time resistivity is generally reduced everywhere in the soil profile, in both experiments.
- After 2.5 h, the situation observed in the two experiments is radically different. In particular, a strong increase in resistivity (about 150%) is observed in the May experiment at a depth between 0.3 m and 0.4 m. This is the region where RWU is expected, and indeed the 3D spatial pattern of this increasing resistivity region is consistent with the expected location of the active roots (see Fig. 7). In November this increasing resistivity region is totally absent, and this corroborates the interpretation that this in May is an effect of RWU, as in November root activity is expected to be much lower than in May. However a certain resistivity increase is localized deeper in the profile. The intensity of the resistivity increase is lower (less than 130%) but still clearly measurable. A reconsideration of the May data show, however, that a similar signal is also present in that experiment, at a depth ranging around 0.8 m and with an

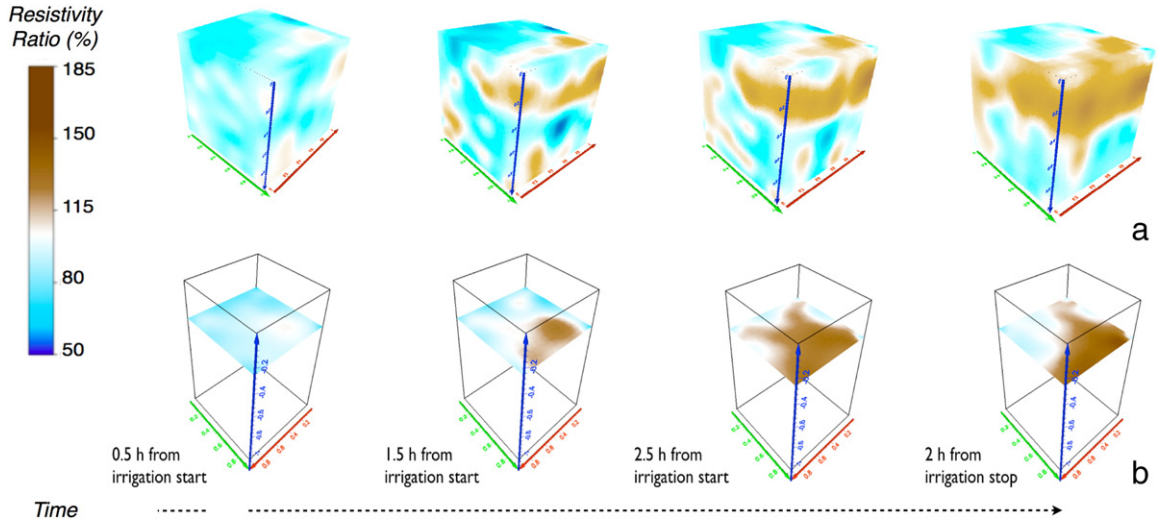

Fig. 6. May 2012 experiment. a) Scatter plot of the volume of interest for 4 time steps during irrigation b) resistivity ratio with respect to background at four time steps shown on the horizontal slice at 30 cm depth.

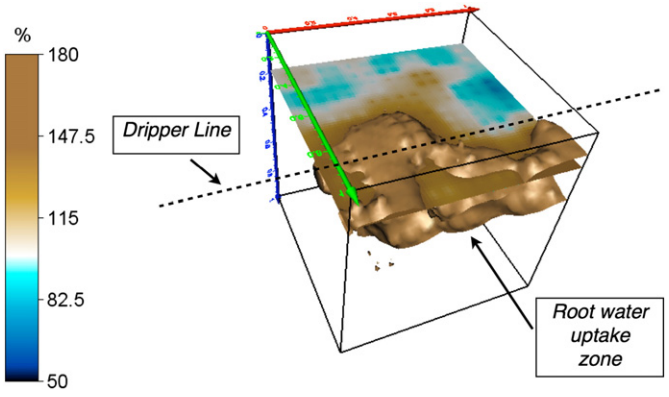

Fig. 7. May 2012 experiment: isosurface corresponding to 150% resistivity ratio with respect to background at 8.5 h since the start of the irrigation experiment.

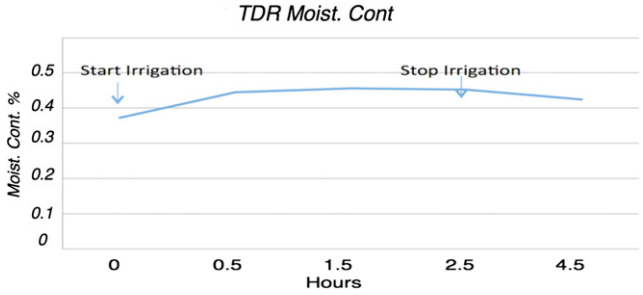

Fig. 9. Moisture content measured by TDR in the top 30 cm. Note how the initial moisture content is even higher than in the May 2012 experiment.

intensity around 115%. Therefore we can hypothesize that both in May and November there is one mechanism other than RWU that increases resistivity at depth.

A possible explanation for this second mechanism of resistivity increase is a sort of piston flow that is pushing fresher irrigated water to a depth where it replaces local pore water, made more saline by a longer contact time with the soil itself. In both the May and November experiments the large volume of irrigated water (500 l) must indeed displace a substantial fraction of the existing water in the system, considering that the ERT control volume is about 0.9 m^3, and porosity was measured in the lab to be around 50%. While quantitatively the piston flow phenomenon is different in May and November, for the different irrigation rate and the different initial water content, as well as for the effect of RWU in May, we expect that in both cases it can be active. Similar piston flow phenomena have been observed elsewhere and are reported in the literature (e.g. Winship et al., 2006; Cassiani et al., 2006; Ursino et al., 2014) and greatly contribute to complicate the interpretation of infiltration in the shallow vadose zone, as observed resistivity changes cannot be attributed, in general, to soil moisture content changes alone.

In order to relate quantitatively the measured resistivity values to water saturation we tested soil samples in the laboratory, making electrical resistivity measurements at several steps of saturation, thus also deriving the pressure–saturation relationship. The soil samples were extracted from a core drilled 1 m away from the ERT installation, and taken from a maximum depth of 60 cm. The average porosity of these samples is 50%. Given the absence of clay in the samples, we elected to model the laboratory results using the classical Archie's (1942) model, obtaining a Formation Factor F = 1.75 and a saturation exponent n = 1.5. As all our resistivity results are given in terms of ratios with respect to background, the use of Archie's law is particularly beneficial given its functional form that allows computing saturation ratios directly from resistivity ratios. We applied the calibrated Archie's law to convert the inverted results of the August 2011 and May 2012 irrigation experiments. As for the November 2012 experiment we deemed that possible soil salinity effects would be important enough to make the conversion of resistivity changes into moisture content changes alone practically meaningless.

The results relevant to the May 2012 are particularly interesting. First of all, the conversion from ERT data into moisture content changes is fully consistent with the changes measured by TDR in the top 30 cm. This corroborates the conversion provided via Archie's law using field evidence. A second, possible more important point, is that the quantification allowed by Archie's law calibration allows an overall water mass balance in the system. In this respect, care must be taken when converting ERT results into estimates of moisture content or solute concentration, as inverted geophysical data may bring with them enough distortion of the true physical parameter field (Day-Lewis et al., 2005) as to induce violations of elementary physical principles, such as mass balance during tracer test monitoring experiments (e.g. Singha and Gorelick, 2005). However, the geometry we are considering here is very effective to reconstruct the mass balance of irrigated water, as this comes as a quasi-one dimensional infiltration front from the top, where in addition electrodes are located. The geometry is similar to the one used, e.g., Koestel et al. (2008) where mass balance was verified by comparison against very detailed TDR data collected in a lysimeter.

Fig. 13 shows the estimated total water content within the ERT control volume (in liters) as a function of time for the May 2012 experiment, taking into account that the monitored 3D volume is equal to roughly 0.9 m^3. This graph shows that, just after the start of the irrigation, the estimated total water volume grows quickly, but it starts to decay well before the end of irrigation. In terms of mass balance, recall that we injected 500 l of water, which shall be compared with the peak of 320 l found to be resident in the ERT control volume at the peak of total saturation (Fig. 10) and with the peak excess 30 l observed

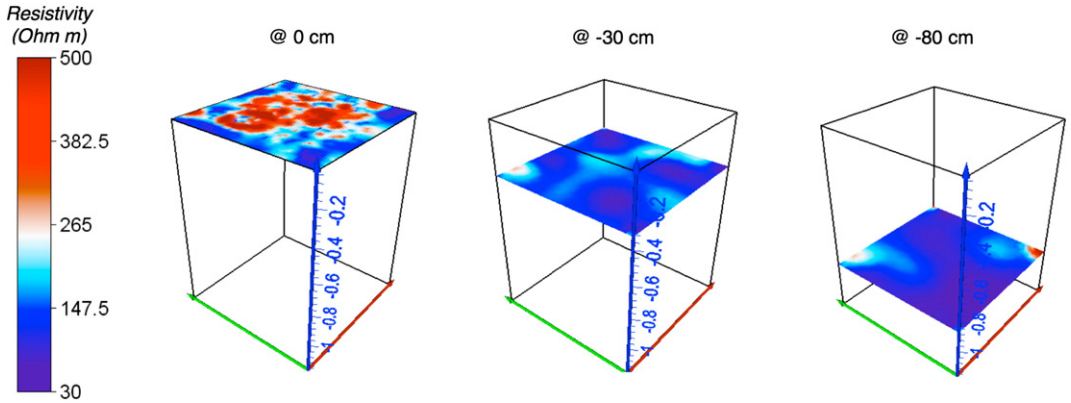

Fig. 8. November 2012 experiment ERT inversion results of the pre-irrigation step for the horizontal slices at 0, 30 and 80 cm depth.

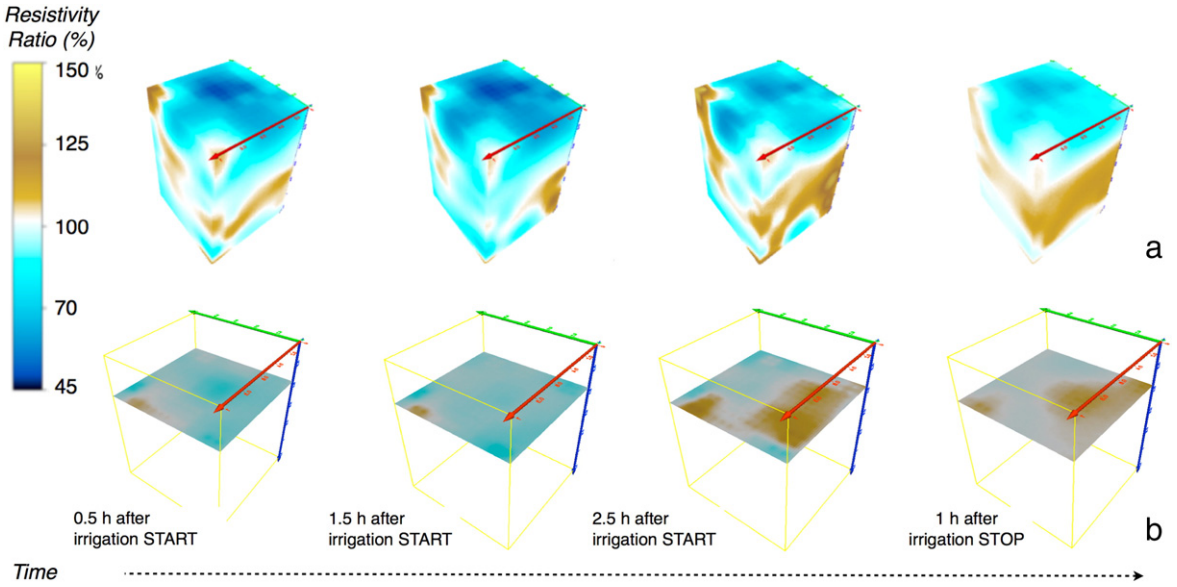

Fig. 10. November 2012 experiment. a) Resistivity ratio with respect to background at four time steps. b): Resistivity ratio with respect to background at four time steps shown on the horizontal slice at 30 cm depth.

in the same graph above the 290 l background value. This comparison shows very clearly that we are considering an open system, where a substantial amount of through-going flow is to be considered to honor mass balance, in addition to the water abstracted by RWU which is definitely an important amount. A quantitative assessment of the system's behavior definitely calls for a distributed hydrological model for a quantitative interpretation of the experiment.

In an attempt to gain some fundamental insight into the processes that can help explain the observed phenomena, we set up a simplified and yet informative modeling exercise. For this purpose we used a 3D Richards' equation solver that is part of the more general code CATHY (Camporese et al., 2010). We constructed a 3D mesh representing the soil volume affected by the irrigation tests, thus much larger than the ERT control volume. We restricted ourselves to modeling the system as homogeneous. While this approach can be limiting when trying to understand the small scale details of the system's behavior, it can be considered adequate if we only aim at understanding the general features of the observed phenomena.

In order to model the unsaturated system behavior, a minimal set of parameters needs to be identified. We used a classical Van Genuchten (1980) parameterization. The collected soil samples were tested in the lab to identify also the relevant hydraulic parameters, including saturated hydraulic conductivity. The average parameters are: saturated hydraulic conductivity $K_s = 6 \times 10^{-5}$ m/s; Van Genuchten's n = 1.35; porosity = 0.5; residual moisture content $\theta_r = 8 \times 10^{-2}$; Van Genuchten's $1/\alpha = 0.7$ m. In particular we verified that the K_s value above is compatible with the observed infiltration observed in the August 2011 experiment, assuming infiltration driven mainly by gravity.

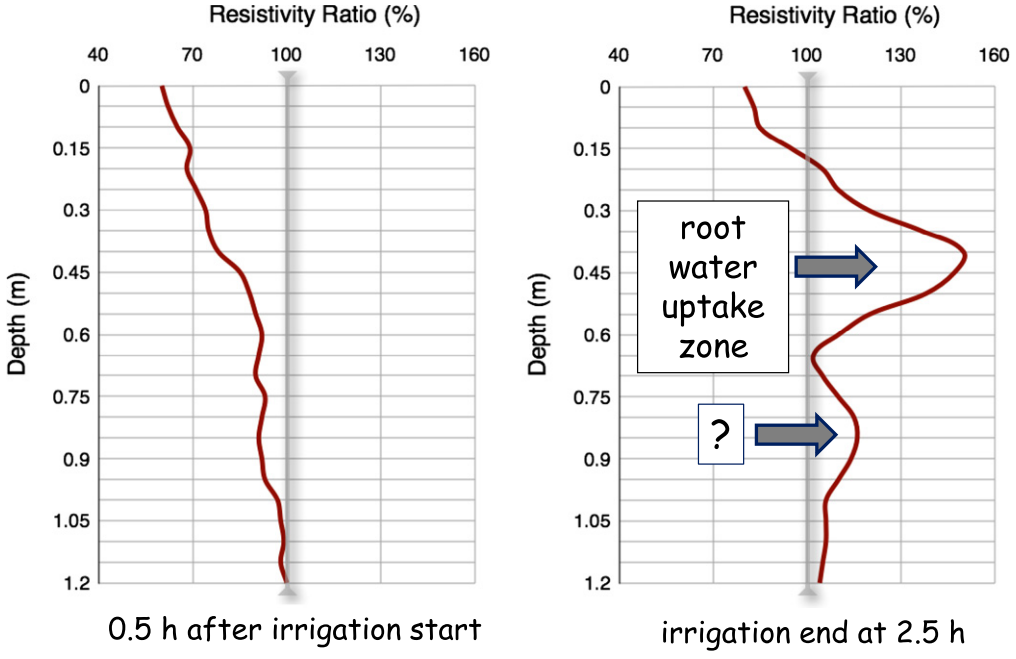

Fig. 11. May 2012 experiment: resistivity changes with respect to background averaged along horizontal planes to give one-dimensional profiles with depth, at two time steps. The marked differences in the two profiles are discussed in the text.

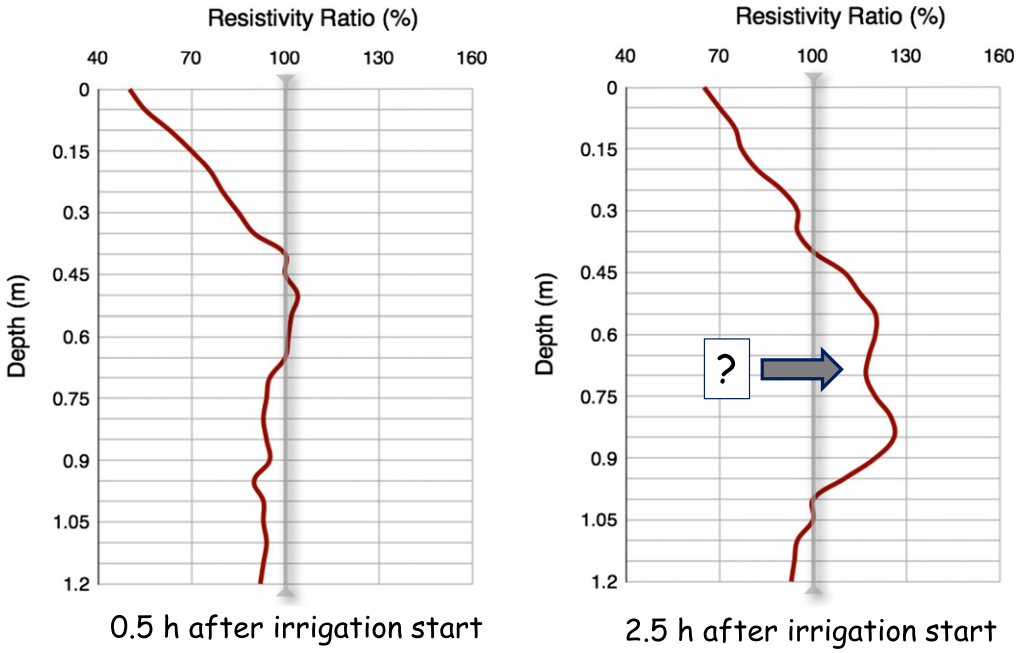

Fig. 12. November 2012 experiment: resistivity changes with respect to background averaged along horizontal planes to give one-dimensional profiles with depth, at two time steps. The marked differences in the two profiles, and the differences with respect to the May 2012 results (Fig. 11) are discussed in the text.

Fig. 14 shows 2D vertical sections cut across the center of the simulated 3D volume, using as an upper boundary condition the flow rate corresponding to the May 2012 experiment. Note that in this numerical simulation we neglected the amount of water removed by RWU, for which we should have had more detailed information e.g. from sap flow measurements (consider e.g. Cassiani et al., 2015). This approximation limits our capability of modeling the details of the experiment, but we deemed the simulations can still be useful to corroborate the possible explanation for the second electrical resistivity increase region observed both in the May and November field data. In Fig. 11 we show, together with the saturation values along the vertical section, also the location of the first particle of water infiltrated from the surface, i.e. the water that was irrigated at time zero. All the saturation increase deeper than the location of this particle is indeed only caused by displacement (piston flow) of the water already resident in the system at the start of the experiment. The most informative result of this simulation is that at time 2.5 h the "new" water has indeed reached the depth where the deeper increase in resistivity is observed, i.e. around 0.8 m from the ground surface, and has not gone any deeper. Considering that no specific calibration of the model has been performed to achieve this result, we believe that this information is particularly strong in corroborating the interpretation of the deeper electrical resistivity increase peak, that is therefore likely to be linked to the displacement of "old" more saline water with "new" fresher water (with electrical conductivity in the range of 240 μS/cm) irrigated at the surface.

6. Conclusions

In this study we aimed at devising a small scale investigation strategy that can provide detailed information concerning the soil–plant interaction mechanisms with particular reference to water mass balance and flows. The methodology makes use of three-dimensional high-resolution electrical resistivity tomography with time-lapse measurements. In particular we found particularly informative the monitoring of irrigation experiments, where time-intensive acquisition was possible and the system was strongly stressed from the hydraulic viewpoint. The evidence collected during three irrigation experiments in an apple orchard points consistently towards some conclusions and poses at the same time a number of questions that will require in-depth analysis and modeling to be answered. The conclusions are:

(a) we showed that a small scale in situ 3D ERT system is capable of monitoring the time-lapse evolution of soil resistivity with sufficient accuracy and resolution as to provide high value data for the understanding of soil–plant systems.

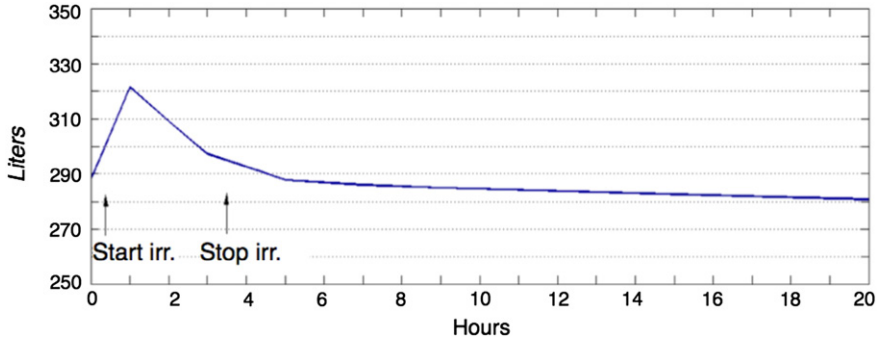

Fig. 13. May 2012 experiment: water mass balance in the ERT control volume estimated from resistivity values according to the lab-calibrated Archie's law relationship.

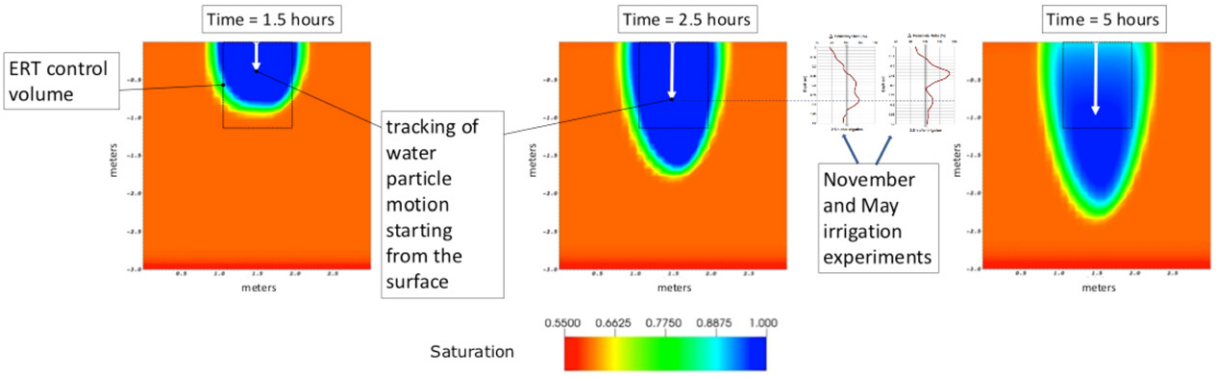

Fig. 14. Vertical sections cut across the simulated 3D volume, relevant to the May 2012 irrigation experiment. Simulations were performed using a Richards' equation simulator (CATHY — Camporese et al., 2010).

(b) from a qualitative viewpoint, this monitoring highlights some key mechanisms of the evolution of soil moisture under external forcings such as irrigation and plant-driven evapotranspiration.
(c) one of the key mechanisms highlighted by our preliminary results is the existence of a clear feedback between the application of a certain irrigation system and the consequent development of the plant root apparatus. In the case of the observed apple tree, drip irrigation causes the roots to develop in a shallow region aligned with the dripper line.

Some of the intricacies inherent in the use of ERT monitoring also became apparent, and in particular:

(d) soil resistivity depends on soil moisture as much as on pore water resistivity, and a mixture of the two dependencies is clearly observed in the field, particularly when abundant fresh water is poured in a system where pore-water (old water) has had the time to equilibrate its salinity with the existing soil mineralogy.
(e) the straight quantification of water mass balance on the basis of ERT results must take into account the open nature of the considered systems, where the amount of flowing mass can exceed the volume of resident water.

Points (d) and (e), however, can be viewed also as challenges towards a more complete and more interesting exploitation of the information content that this type of monitoring can provide. This will require coupling modeling and monitoring well beyond the simple exercise shown in this paper. In particular, we see Data Assimilation techniques (e.g. Manoli et al., 2015) as key instruments to couple the spatially extensive and time intensive data obtained from traditional and innovative minimally invasive techniques with mechanistic models representing the soil moisture dynamics and root water uptake (RWU), whole plant transpiration, and leaf-level photosynthesis (e.g. Manoli et al., 2014). This is by no means a totally novel approach in the context of hydro-geophysical research (consider e.g. Hinnell et al., 2010 for a review). However, new challenges and promising pathways will surely stem from the use of Data Assimilation techniques to small scale, plant related applications.

Acknowledgments

We acknowledge financial support from the EU FP7 project CLIMB "Climate Induced Changes on the Hydrology of Mediterranean Basins", grant agreement no. 244151.

References

al Hagrey, S.A., Petersen, T., 2011. Numerical and experimental mapping of small root zones using optimized surface and borehole resistivity tomography. Geophysics 76 (2). http://dx.doi.org/10.1190/1.3545067.671.
Amato, M., Basso, B., Celano, G., Bitella, G., Morelli, G., Rossi, R., 2008. In situ detection of tree root distribution and biomass by multi-electrode resistivity imaging. Tree Physiol. 28, 1441–1448.
Anderson, S.P., Blum, J., Brantley, S.L., Chadwick, O., Chorover, J., Derry, L.A., Drever, J.I., Hering, J.G., Kirchner, J.W., Kump, L.R., Richter, D., White, A.F., 2004. Proposed initiative would study Earth's weathering engine. EOS Trans. 85 (28), 265–269 (American Geophysical Union).
Archie, G.E., 1942. The Electrical Resistivity Log as an Aid in Determining Some Reservoir.
Bassuk, N., Grabosky, J., Mucciardi, A., Raffel, G., 2011. Ground-penetrating radar accurately locates tree roots in two soil media under pavement. Arboricult. Urban For. 37 (4), 160–166.
Beff, L., Günther, T., Vandoorne, B., Couvreur, V., Javaux, M., 2013. Three-dimensional monitoring of soil water content in a maize field using Electrical Resistivity Tomography. Hydrol. Earth Syst. Sci. 17 (595–609), 2013. http://dx.doi.org/10.5194/hess-17-595-2013.
Binley, A., 2011. http://www.es.lancs.ac.uk/people/amb/Freeware/freeware.htm (last accessed August 2014).
Binley, A.M., Kemna, A., 2005. DC resistivity and induced polarization methods. In: Rubin, Y., Hubbard, S.S. (Eds.), Hydrogeophysics. Water Sci. Technol. Library, Ser. 50. Springer, New York, pp. 129–156.
Binley, A., Shaw, B., Henry-Poulter, S., 1996. Flow pathways in porous media: electrical resistance tomography and dye staining image verification. Meas. Sci. Technol. 7 (3), 384–390.
Binley, A.M., Cassiani, G., Middleton, R., Winship, P., 2002. Vadose zone flow model parameterisation using cross-borehole radar and resistivity imaging. J. Hydrol. 267, 147–159 (characteristics. Transactions of the American Institute of Mining Engineers, 146, 54–62).
Binley, A.M., Cassiani, G., Deiana, R., 2011. Hydrogeophysics — opportunities and challenges. Boll. Geofis. Teor. Appl. 51 (4), 267–284.
Boaga, J., D'Alpaos, A., Cassiani, G., Marani, M., Putti, M., 2014. Plant–soil interactions in salt-marsh environments: experimental evidence from electrical resistivity tomography (ERT) in the Venice lagoon. Geophys. Res. Lett. 41, 6160–6166. http://dx.doi.org/10.1002/2014GL060983.
Bonan, G., 2002. Ecological Climatology. Cambridge University Press 0521800323 (690 pages, 41 color plates, 68 tables, 330 figures, 14 chapters).
Brantley, S.L., White, T.S., White, A.F., Sparks, D., Richter, D., Pregitzer, K., Derry, L., Chorover, J., Chadwick, O., April, R., Anderson, S., Amundson, R., 2006. Frontiers in Exploration of the Critical Zone, an NSF-sponsored workshop, 30 pp. National Science Foundation, Washington, D.C.
Butnor, J.R., Doolittle, J.A., Kress, L., Cohen, S., Johnsen, K.H., 2001. Use of ground-penetrating radar to study tree roots in the southeastern United States. Tree Physiol. 21, 1269–1278.
Camporese, M., Paniconi, C., Putti, M., Orlandini, S., 2010. Surface-subsurface flow modeling with path-based runoff routing, boundary condition-based coupling, and assimilation of multisource observation data. Water Resour. Res. 46, W02512.
Camporese, M., Salandin, P., Cassiani, G., Deiana, R., 2011. Impact of ERT data inversion uncertainty on the assessment of local hydraulic properties from tracer test experiments. Water Resour. Res. 47 (W12508), 2011. http://dx.doi.org/10.1029/2011WR010528.
Camporese, M., Cassiani, G., Deiana, R., Salandin, P., Binley, A.M., 2014. Comparing coupled and uncoupled hydrogeophysical inversions using ensemble Kalman filter assimilation of ERT-monitored tracer test data. Water Resour. Res. (in press).
Cassiani, G., Bruno, V., Villa, A., Fusi, N., Binley, A.M., 2006. A saline tracer test monitored via time-lapse surface electrical resistivity tomography. J. Appl. Geophys. 59, 244–259. http://dx.doi.org/10.1016/j.jappgeo2005.10.007.
Cassiani, G., Godio, A., Stocco, S., Villa, A., Deiana, R., Frattini, P., Rossi, M., 2009. Monitoring the hydrologic behaviour of steep slopes via time-lapse electrical resistivity

tomography. Near Surf. Geophys. 475–486 http://dx.doi.org/10.3997/1873-0604.2009013 (special issue on Hydrogeophysics – Methods and Processes).
Cassiani, G., Ursino, N., Deiana, R., Vignoli, G., Boaga, J., Rossi, M., Perri, M.T., Blaschek, M., Duttmann, R., Meyer, S., Ludwig, R., Soddu, A., Dietrich, P., Werban, U., 2012. Non-invasive monitoring of soil static characteristics and dynamic states: a case study highlighting vegetation effects. Vadose Zone J. 11. http://dx.doi.org/10.2136/2011.0195 (vzj2011.0195, Special Issue on SPAC - Soil-plant interactions from local to landscape scale, August).
Cassiani, G., Boaga, J., Vanella, D., Perri, M.T., Consoli, S., 2015. Monitoring and modelling of soil–plant interactions: the joint use of ERT, sap flow and Eddy Covariance data to characterize the volume of an orange tree root zone. Hydrol. Earth Syst. Sci. Discuss. 11, 13353–13384. http://dx.doi.org/10.5194/hessd-11-13353-2014 (www.hydrol-earth-syst-sci-discuss.net/11/13353/2014/).
Daily, W.A., Ramirez, D. LaBrecque, Nitao, J., 1992. Electrical resistivity tomography of vadose water movement. Water Resour. Res. 28 (5), 1429–1442.
Day-Lewis, F.D., Singha, K., Binley, A.M., 2005. Applying petrophysical models to radar travel time and electrical resistivity tomograms: resolution-dependent limitations. J. Geophys. Res. Solid Earth 110 (B8), B08206.
De Silva, H.N., Hall, A.J., Tustin, D.S., Gandar, P.W., 1999. Analysis of distribution of root length density of apple trees on different dwarfing rootstocks. Ann. Bot. 83 (4), 335–345.
Deiana, R., Cassiani, G., Kemna, A., Villa, A., Bruno, V., Bagliani, A., 2007. An experiment of non invasive characterization of the vadose zone via water injection and cross-hole time-lapse geophysical monitoring. Near Surf. Geophys. 5, 183–194 (3 June).
Easterling, D.R., Meehl, G.A., Parmesan, C., Changnon, S.A., Karl, T.R., Mearns, L.O., 2000. Climate extremes: observations, modeling, and impacts. Science 2068 (2000), 289. http://dx.doi.org/10.1126/science.289.5487.2068.
Falkenmark, M., Rockstro¨m, J., 2004. Balancing water for humans and nature. The New Approach in Ecohydrology. Earthscan, London (247 pp.).
Hinnell, A.C., Ferré, T.P.A., Vrugt, J.A., Huisman, J.A., Moysey, S., Rings, J., Kowalsky, M.B., 2010. Improved extraction of hydrologic information from geophysical data through coupled hydrogeophysical inversion. Water Resour. Res. 46, W00D40. http://dx.doi.org/10.1029/2008WR007060.
Howden, S.M., Soussana, J.F., Tubiello, F.N., Chhetri, N., Dunlop, M., Meinke, H., 2007. Adapting agriculture to climate change. PNAS 104 (no. 50). http://dx.doi.org/10.1073/pnas.0701890104.
Jayawickreme, H., Van Dam, R., Hyndman, D.W., 2008. Subsurface imaging of vegetation, climate, and root-zone moisture interactions. Geophys. Res. Lett. 35, L18404. http://dx.doi.org/10.1029/2008GL034690.
Jayawickreme, D.H., Van Dam, R.L., Hyndman, D.W., 2010. Hydrological consequences of land-cover change: quantifying the influence of plants on soil moisture with time-lapse electrical resistivity. Geophysics 75 (NO. 4), WA43–WA50. http://dx.doi.org/10.1190/1.3464760 (JULY-AUGUST 2010).
Jayawickreme, D.H., Jobbágy, E.G., Jackson, Robert B., 2014. Geophysical subsurface imaging for ecological applications. New Phytol. 201, 1170–1175. http://dx.doi.org/10.1111/nph.12619.
Koestel, J., Kemna, A., Javaux, M., Binley, A., Vereecken, H., 2008. Quantitative imaging of solute transport in an unsaturated and undisturbed soil monolith with 3-D ERT and TDR. Water Resour. Res. 44, W12411. http://dx.doi.org/10.1029/2007WR006755.
Leucci, G., 2010. The use of three geophysical methods for 3D images of total root volume of soil in urban environments. Explor. Geophys. 2010 (41), 268–278. http://dx.doi.org/10.1071/EG09034.
Ludwig, R., Soddu, A., Duttmann, R., Baghdadi, N., Benabdallah, S., Deidda, R., Marrocu, M., Strunz, G., Wendland, F., Engin, G., Paniconi, C., Prettenthaler, F., Lajeunesse, I., Afifi, S., Cassiani, G., Bellin, A., Mabrouk, B., Bach, H., Ammerl, T., 2010. Climate-induced changes on the hydrology of Mediterranean basins — a research concept to reduce uncertainty and quantify risk. Fresenius Environ. Bull. 19 (10A) (Sp. Iss. SI, 2379-2384).
Macleod, C.J.A., Humphreys, M.W., Whalley, W.R., Turner, L., Binley, A., Watts, C.W., Skøt, L., Joynes, A., Hawkins, S., King, I.P., O'Donovan, S., Haygarth, P.M., 2013. A novel grass hybrid to reduce flood generation in temperate regions. Sci. Rep. 3, 1683. http://dx.doi.org/10.1038/srep01683.
Manoli, G., Bonetti, S., Domec, J.C., Putti, M., Katul, G., Marani, M., 2014. Tree root systems competing for soil moisture in a 3D soil–plant model. Adv. Water Resour. 66, 32–42. http://dx.doi.org/10.1016/j.advwatres.2014.01.006.
Manoli, G., Rossi, M., Pasetto, D., Deiana, R., Ferraris, S., Cassiani, G., Putti, M., 2015. An iterative particle filter approach for coupled hydro-geophysical modeling and inversion of a controlled infiltration experiment. J. Comput. Phys. 37–51. http://dx.doi.org/10.1016/j.jcp.2014.11.035.
Michot, D., Benderitter, Y., Dorigny, A., Nicoullaud, B., King, D., Tabbagh, A., 2003. Spatial and temporal monitoring of soil water content with an irrigated corn crop cover using surface electrical resistivity tomography. Water Resour. Res. 39 (5), 1138. http://dx.doi.org/10.1029/2002WR001581.
Nijland, W., van der Meijde, M., Addink, E.A., de Jong, S.M., 2010. Detection of soil moisture and vegetation water abstraction in a Mediterranean natural area using electrical resistivity tomography. Catena 81 (2010), 209–216. http://dx.doi.org/10.1016/j.catena.2010.03.005.
Petersen, T., al Hagrey, S.A., 2009. Mapping root zones of small plants using surface and borehole resistivity tomography. Lead. Edge 1220–1224.
Robinson, J.L., Slater, L.D., Schäfer, K.V.R., 2012. Evidence for spatial variability in hydraulic redistribution within an oak–pine forest from resistivity imaging. J. Hydrol. 430–431 (2012), 69–79. http://dx.doi.org/10.1016/j.jhydrol.2012.02.002.
Rodriguez-Iturbe, I., Porporato, A., 2005. Ecohydrology of Water controlled Ecosystems: Soil Moisture and Plant Dynamics. Cambridge University Press, New York.
Rossi, R., Amato, M., Bitella, G., Bochicchi, R., Ferreira Gomes, J.J., Lovelli, S., Martorella, E., Favale, P., 2011. Electrical resistivity tomography as a non-destructive method for mapping root biomass in an orchard. Eur. J. Soil Sci. 62, 206–215. http://dx.doi.org/10.1111/j.1365-2389.2010.01329.x (April).
Shanahan, P.W., Binley, A., Whalley, W.R., Watts, C.W., 2015. The use of electromagnetic induction to monitor changes in soil moisture profiles beneath different wheat genotypes. Soil Sci. Soc. Am. J. 79, 459–466. http://dx.doi.org/10.2136/sssaj2014.09.0360.
Singha, K., Gorelick, S.M., 2005. Saline tracer visualized with three dimensional electrical resistivity tomography: field-scale spatial moment analysis. Water Resour. Res. 41, W05023. http://dx.doi.org/10.1029/2004WR003460.
Tilman, D., Fargione, J., Wolff, B., D'Antonio, C., Dobson, A., Howarth, R., Schindler, D., Schlesinger, W.H., Simberloff, D., Swackhamer, D., 2001. Forecasting Agriculturally Driven Global Environmental Change Science. 292 (no. 5515), 281–284. http://dx.doi.org/10.1126/science.1057544.
U.S. National Research Council Committee on Basic Research Opportunities in the Earth Sciences, 2001. Basic Research Opportunities in the Earth Sciences. National Academies Press, Washington, D.C.
Ursino, N., Cassiani, G., Deiana, R., Vignoli, G., Boaga, J., 2014. Measuring and modelling water related soil–vegetation feedbacks in a fallow plot. Hydrol. Earth Syst. Sci. http://dx.doi.org/10.5194/hess-18-1105-2014.
Van Genuchten, M.T., 1980. A closed form equation for predicting the hydraulic conductivity of unsaturated soils. Soil Sci. Soc. Am. J. 44, 892–898.
Vereecken, H., Binley, A., Cassiani, G., Kharkhordin, I., Revil, A., Titov, K. (Eds.), 2006. Applied Hydrogeophysics. Springer-Verlag, Berlin.
Werban, U., al Hagrey, S.A., Rabbel, W., 2008. Monitoring of root-zone water content in the laboratory by 2D geoelectrical tomography. J. Plant Nutr. Soil Sci. 171 (6), 927–935. http://dx.doi.org/10.1002/jpln.200700145. 781.
Wiley, M.J., Hyndman, D.W., Pijanowski, B.C., Kendall, A.D., Riseng, C., Rutherford, E.S., Cheng, S.T., Carlson, M.L., Tyler, J.A., Stevenson, R.J., Steen, P.J., Seelbach, P.W., Koches, J.M., Rediske, R.R., 2010. A multi-modeling approach to evaluating climate and land use change impacts in a Great Lakes River Basin. Hydrobiologia. http://dx.doi.org/10.1007/s10750-010-0239-2.
Winship, P., Binley, A., Gomez, D., 2006. Flow and transport in the unsaturated Sherwood Sandstone: characterization using cross-borehole geophysical methods. In: Barker, Tellam (Eds.), Fluid Flow and Solute Movement in Sandstones: The Onshore UK Permo-Triassic Red Bed Sequence. Geological Society, London, Special Publications 263, pp. 219–231.
Wu, Y., Guo, L., Cui, X., Chen, J., Cao, X., Lin, H., 2014. Ground-penetrating radar-based automatic reconstruction of three-dimensional coarse root system architecture. Plant Soil. http://dx.doi.org/10.1007/s11104-014-2139-0.